Full-potential LAPW calculation of electron momentum density and related properties of Li

Tunna Baruah, Rajendra R. Zope, and Anjali Kshirsagar*
Department of Physics, University of Pune, Pune-411007, India
(Received 2 November 1998; revised manuscript received 1 June 1999)

Electron momentum density and Compton profiles in lithium along ⟨100⟩, ⟨110⟩, and ⟨111⟩ directions are calculated using full-potential linear augmented plane-wave basis within the generalized gradient approximation. The profiles have been corrected for correlations with the Lam-Platzman formulation using self-consistent charge density. The first and second derivatives of the Compton profiles are studied to investigate the Fermi-surface breaks. Decent agreement is observed between recent experimental values and our calculated values. Our values for the derivatives are found to be in better agreement with experiments than earlier theoretical results. The two-photon momentum density and one- and two-dimensional angular correlations of positron annihilation radiation are also calculated within the same formalism, and include the electron-positron enhancement factor. [S0163-1829(99)06139-1]

I. INTRODUCTION

Compton scattering and positron annihilation techniques are well-established tools for studying the momentum distribution of electrons in solids.[1–4] In the Compton scattering technique, the intensity distribution of energy-broadened Compton-scattered radiation (called the Compton profile) is studied, while in the positron annihilation technique measurement is performed of the angular correlation between two photons emitted during the annihilation of a thermalized positron with electrons in the solid. The Compton profile (CP) and angular correlation of positron annihilation radiation (ACPAR) curves contain the fingerprints of Fermi-surface (FS) breaks in the momentum distribution in the first and higher Brillouin zones. It is well known that although the magnitude of the discontinuity in the momentum distribution itself changes due to electron-electron, electron-ion, and electron-positron correlations, the position of the discontinuity remains unchanged.[5–7] Thus, these techniques together are useful to extract information about FS geometry, and to identify electron correlation effects. Positron annihilation techniques are more sensitive to the outer, weakly bound conduction electrons, and are also capable of performing measurements in both one- and two-dimensional geometries, with much superior momentum resolution. Theoretically, however, it is more straightforward to calculate CP's, as ACPAR studies necessitate accounting for electron-positron many-body correlation effects. These effects are incorporated in the form of momentum-, energy-, or density-dependent enhancement factors.[8–12]

Early measurements of the Compton profile suffered from limited momentum resolution in the Compton scattering experiment (~0.4 a.u.). The advent of high-intensity, high-energy, and well-polarized synchrotron sources, and spectrometers with high resolution (~0.12 a.u.), have resulted in a revival of interest in this area.[13–15] On the theoretical side, high-performance computing facilities have made it possible to perform calculations on a fine **p** mesh, with a better convergence criteria for the total energy and charge-density self-consistency.

In the present paper, we report full-potential linearized augmented plane-wave (FP-LAPW) calculations of the electron momentum distribution in Li. In lithium, because of its smallness, the electron-ion interactions are strong and the electrons do not behave like a textbook example of a homogeneous electron gas as in sodium. The Fermi surface of Li shows a small but definite departure from the free-electron sphere. The electron momentum density (EMD) is highly anisotropic, and the high-momentum components (HMC's) are small but important. The momentum distribution of Li has been investigated in the past, both theoretically and experimentally, by several workers[16–20] with available state-of-the-art procedures. Recently, Sakurai *et al.*[13] performed high-resolution Compton scattering experiments for Li to measure Compton profiles and Fermi radii. The measured CP's are compared with the theoretical ones calculated using the Korringa-Kohn-Rostoker (KKR) method. Subsequently, Schülke *et al.*[15] measured 11-directional Compton profiles and employed them to reconstruct the three-dimensional EMD in Li metal. A comparison of the experimental CP's with their theoretical counterparts has always shown some discrepancies. This is partly due to the various approximations involved in computing the profile, and partly due to the experimental errors. Methods like FP-LAPW can provide accurate results for the one-electron wave function, and hence should be employed for computation of theoretical CP's. Such accurate calculations of the CP's of Li have been reported by Kubo[21,22] employing the *GW* approximation using FP-LAPW wave functions within the local-density approximation (LDA) as the zeroth approximation. The calculated CP's are in good agreement with the experimental values, but the derivatives of the CP's match the experimental ones poorly.[21] The derivatives of CP's are important as they provide information about the Fermi surface.

In the present paper, we use the full-potential linearized augmented-plane wave method for the computation of CP's which have been corrected to include the correlation effects not accounted for within the LDA, along with one- and two dimensional angular correlations of positron annihilation radiation, which include corrections due to electron-positron correlation effects. Such studies using the same formalism for calculation of CP and ACPAR can provide complemen-

tary information about the Fermi surface and the electron momentum distribution. Our aim in this paper is to extract the FS geometry from the two techniques together, and to identify the part of electron correlations left out in the theory to describe the EMD. The plan of the paper is as follows: in Sec. II, we present the momentum space formulation of the LAPW wave function, and computational details, while Sec. III deals with the results.

II. METHODOLOGY AND COMPUTATIONAL DETAILS

The one-electron wave function for an electron in the state labeled by wave vector $\mathbf{k}$ and band index j is expanded in the LAPW basis $\phi_{\mathbf{k}+\mathbf{G}}(\mathbf{r})$ as

$$\psi^j_{\mathbf{k}}(\mathbf{r}) = \sum_{\mathbf{G}} c^j_{\mathbf{k}+\mathbf{G}} \phi_{\mathbf{k}+\mathbf{G}}(\mathbf{r}), \tag{1}$$

where $c^j_{\mathbf{k}+\mathbf{G}}$ are the expansion coefficients, and $\mathbf{G}$ denotes the reciprocal-lattice vector. The LAPW function is a plane wave outside the muffin-tin sphere, while inside it is a linear combination of $u_l(r)$, the solution of the radial Schrödinger equation and its energy derivative $\dot{u}_l(r)$. This allows greater flexibility inside the spheres (than the APW method) and hence permits computation of an accurate solution.[23]

The momentum space LAPW wave function is obtained by a Dirac-Fourier transformation of Eq. (1) and the electron momentum density is computed from the momentum space wave function of occupied states. The Compton profile is then obtained by performing a double integral.

The theoretical Compton profile thus obtained is overestimated at low momenta and is underestimated at higher momentum values than its experimental counterpart. This discrepancy is often attributed to the correlation effects that are ignored in the independent-particle model.[24] Lam and Platzman[24] showed that these effects can be incorporated into the EMD by augmenting a correction term to the independent-electron model momentum density. The recent formulation of Cardwell and Cooper,[25] based on work by Lam and Platzman, which takes care of the nonunity occupation below the Fermi momentum k_f and nonzero occupation beyond k_f, has been employed in the present work.

For a single positron in a defect-free crystal, the positron density will be distributed over the entire crystal. Therefore, the positron wave function $\psi_+(\mathbf{r})$ is considered to be delocalized, and is represented by a plane-wave basis. Further, as the positron essentially thermalizes before annihilation, it is assumed to be in the state $\mathbf{k}_+ = 0$. The enhancement in the two photon momentum density (TPMD) due to the electron-positron short-range correlation is calculated according to the prescription given by Puska *et al.*,[10] which is a function of electron and positron densities. Thus, the TPMD is evaluated using the prescription

$$\rho^{2\gamma}(\mathbf{p}) = \sum_{\mathbf{k},j}^{occ} |F^j_{\mathbf{k}}(\mathbf{p})|^2 = \sum_{\mathbf{k},j}^{occ} \left| \int e^{-i\mathbf{p}\cdot\mathbf{r}} \psi_+(\mathbf{r}) \psi^j_{\mathbf{k}}(\mathbf{r}) \sqrt{g[n^e(\mathbf{r}), n^+(\mathbf{r})]}\, d^3r \right|^2 \tag{2}$$

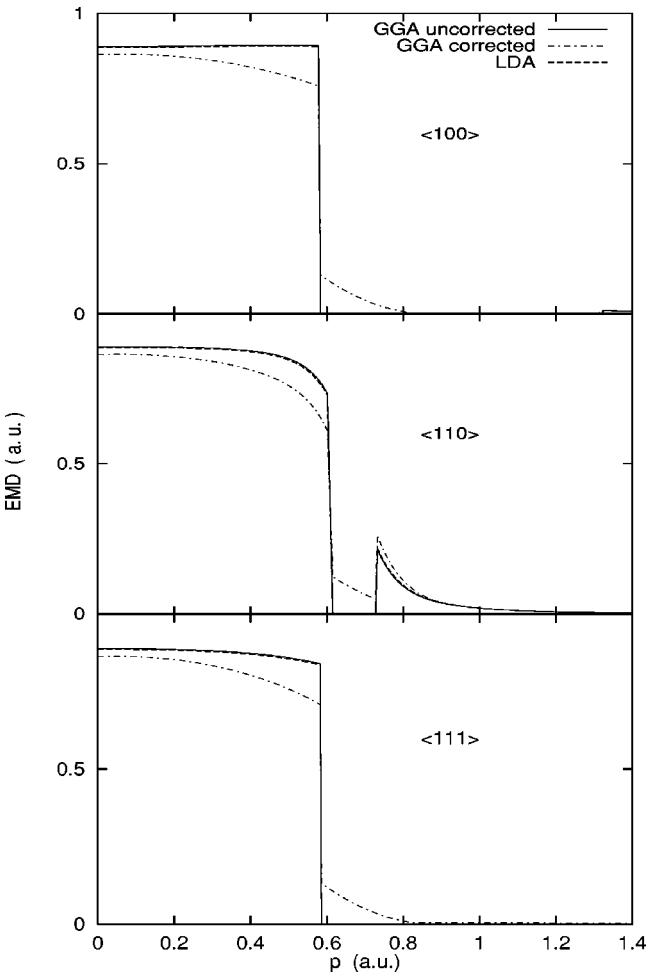

FIG. 1. Electron momentum densities along ⟨100⟩, ⟨110⟩, and ⟨111⟩ directions.

where $n^e(\mathbf{r})$ and $n^+(\mathbf{r})$ are the electron and positron densities, respectively, and the enhancement factor $g[n^e(\mathbf{r}), n^+(\mathbf{r})]$ in the limit $n^+(\mathbf{r}) \to 0$ is

$$g_0(r_s) = 1 + 1.23 r_s + 0.98890 r_s^{3/2} - 1.4820 r_s^2 + 0.3956 r_s^{5/2} + r_s^3/6, \tag{3}$$

where $r_s = [3/4\pi n^e(\mathbf{r})]^{1/3}$.

A self-consistent band-structure calculation was performed using the LAPW method as implemented in the WIEN97 package.[26] The calculation employs a full potential which implies that the nonspherical part of the potential inside the muffin-tin sphere and its deviation from the constant potential in the interstitial region are taken into consideration. The simplified generalized gradient approximation (GGA) due to Perdew *et al.*[27] was used for the exchange-correlation part of the Kohn-Sham potential. In the band-structure calculation the lattice constant of Li in bcc structure is taken to be 6.61375 a.u.[28] The self-consistency cycles were carried out to an energy tolerance of 10^{-6} Ry, and a charge convergence of 10^{-5} electrons. The various band-structure parameters agree very well with earlier accurate calculations.[20,29]

For the calculation of Compton profile, in 1/48th of the Brillouin zone we used 40 425 $\mathbf{k}$ points to evaluate the mo-

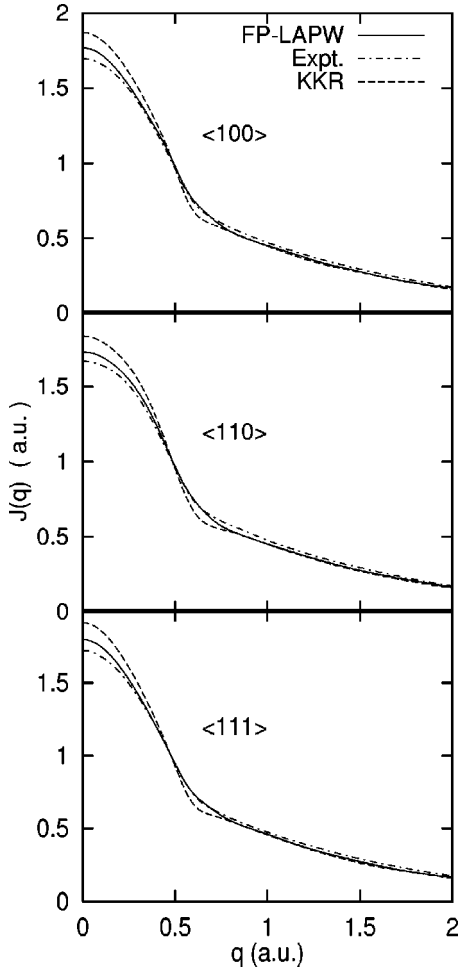

FIG. 2. Compton profiles along ⟨100⟩, ⟨110⟩, and ⟨111⟩ directions.

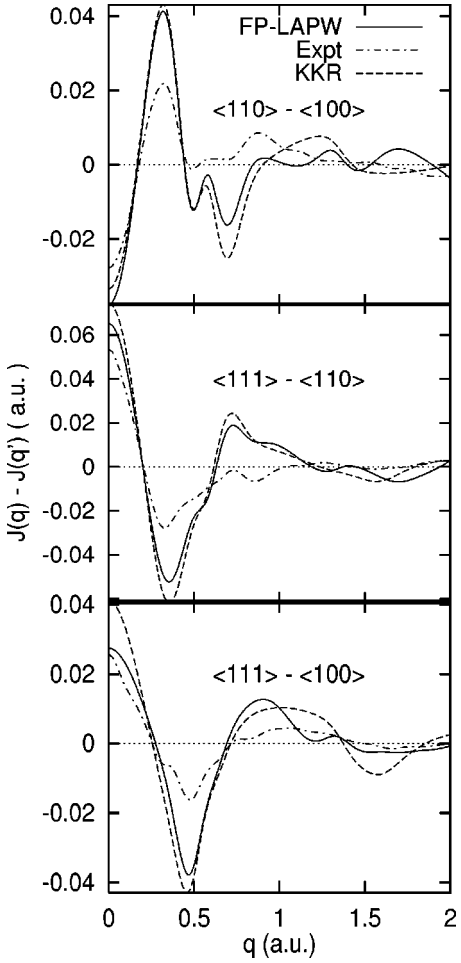

FIG. 3. Anisotropies of the Compton profiles between various directions.

mentum space wave function which when translated by the reciprocal space vectors yield 40425×531 **p** points. The linear tetrahedron method[30] was used for the calculation of Compton profiles over a momentum mesh of 0.001 a.u. The correlation correction was carried out as described by Cardwell and Cooper.[25] In carrying out these calculations we used the self-consistent density inside the muffin-tin sphere, whereas in the interstitial region we assumed the density to be flat with little structure. No r_s cut-off value was used, as suggested by Cardwell and Cooper.[25]

For the calculation of two-photon momentum density, the wave function for the positron was obtained by solving the secular determinant once using the self-consistent Coulombic potential from earlier calculation for electronic band structure but with an opposite sign. We have used 819 **k** points to evaluate $F^j_{\mathbf{k}}(\mathbf{p})$.

III. RESULTS AND DISCUSSION

The electron momentum density for lithium metal along ⟨100⟩, ⟨110⟩, and ⟨111⟩ directions in momentum space is plotted in Fig. 1. Each panel shows the EMD along one direction, calculated within the LDA and GGA employing von Barth-Hedin (VBH)[31] and Perdew-Burke-Ernzerhof (PBE)[27] exchange-correlation potentials, respectively, along with a GGA-EMD corrected using a Lam-Platzman (LP)[24] term in that direction, employing the model momentum density proposed by Cardwell and Cooper.[25] The results are almost identical for VBH and PBE exchange-correlation potentials, indicating that the nonlocal corrections as described within the GGA do not seem to affect the momentum density in Li, although their electronic structure is slightly different in the LDA and GGA. This gives rise to almost identical (CP's) for LDA and GGA formulations, as predicted by Lam and Platzman.[32] These observations for Li support the fact that although the ionic potential is strong in Li, the conduction electron density behaves more like a homogeneous electron gas. Similar calculations for transition metals do show significant differences in LDA and GGA results.[33]

The strong ionic periodic potential, however, does couple the states near Brillouin-zone (BZ) boundaries, and the conduction electron wave functions contain strong high-momentum components and the EMD does show an anisotropic behavior, as is evident from Fig. 1. Since Li has only one electron in the conduction band, in the one-electron picture the EMD is zero beyond k_f in the first BZ and between its images in higher zones. Lam-Platzman[24] correction partly takes care of the correlation effects on the wave functions in the one-electron picture. The occupation number of an interacting homogeneous electron gas is estimated to be smaller than that of a noninteracting free-electron gas by 4% for Li. Our LP-corrected EMD displays the effect of states below

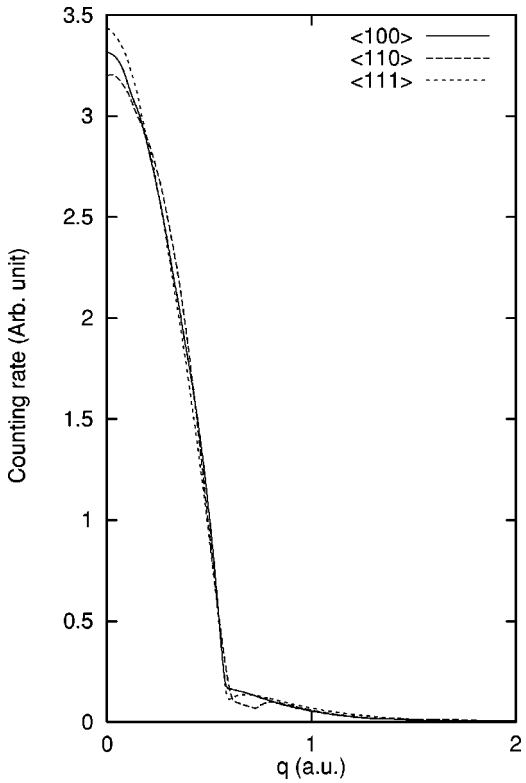

FIG. 4. One-dimensional ACPAR curves along ⟨100⟩, ⟨110⟩, and ⟨111⟩ directions.

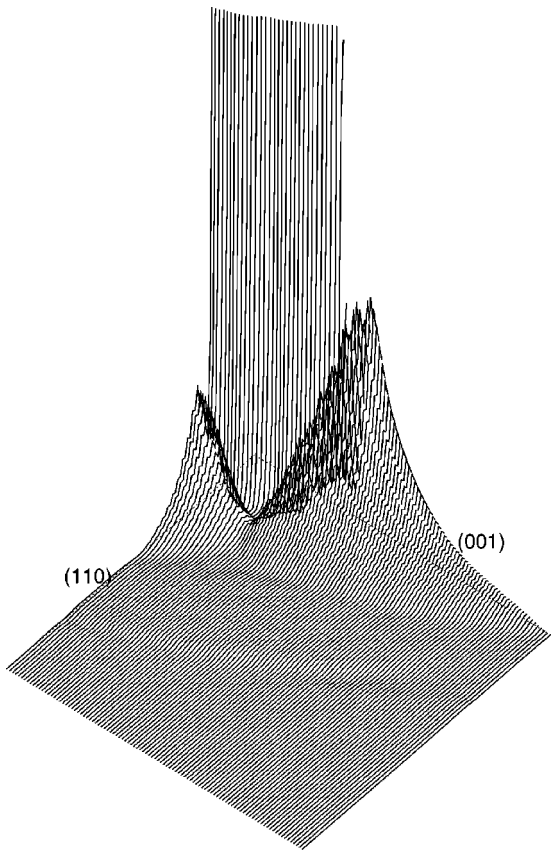

FIG. 5. Two-dimensional ACPAR plot of Li in the $(1\bar{1}0)$ plane.

k_f, being pushed above k_f in Li, and these can be compared with results in Fig. 5 of Ref. 17, which uses mean occupation numbers derived from electron-gas data for correlation effects and couples them with orthogonalized plane-wave band-structure method. EMD dies off in higher zones along ⟨100⟩ and ⟨111⟩ directions, but shows a strong umklapp component along the ⟨110⟩ direction. These higher-momentum components play an important role in determining the shapes of Compton profiles and angular correlation curves.

Compton profiles $J_{\hat{k}}(q)$ corrected for the correlations are presented in Fig. 2 together with the experimental and KKR results[13] with $\hat{k}$ along ⟨100⟩, ⟨110⟩, and ⟨111⟩ directions. In order to facilitate the comparison with experimental CP's, the theoretical CP's were convoluted with a Gaussian with a full width at half maximum (FWHM) of 0.12 a.u. (the experimental resolution was given in Ref. 13). Our Compton profiles, when compared with experimental values, support the widely known behavior, namely, overestimation at low momentum and underestimation at higher momentum values. Correlation corrections lower the CP values within the main Fermi surface but they are still higher than the experimental results. It is to be noted that KKR values are consistently higher than our values near $q=0$, and show a more pronounced cusplike behavior near $\mathbf{k}_f$ for all three directions. The cusp seen in the CP reflects the discontinuity in the EMD at $\mathbf{k}_f$ in the first BZ, and their images in higher zones. The results indicate that the discontinuity is smaller in FP-LAPW calculations than in those of KKR. The disagreement between present results and KKR results could be attributed to the fact that present work is a full-potential calculation whereas KKR used a muffin-tin shape approximation. Second, the LP correction was calculated using the prescription of Cardwell and Cooper,[25] employing self-consistent charge density in the present work, whereas KKR used interpolated results from homogeneous electron-gas data. Our results agree with those of KKR beyond $q=0.8$ a.u., while the experimental values are consistently higher than the theory in this region. This reflects that the nonzero occupation beyond $\mathbf{k}_f$ for the inhomogeneous electron gas is only partially accounted for by the theory.

We have also compared the directional anisotropies in the Compton profiles with the experimental work of Sakurai *et al.*,[13] and the overall agreement is found to be good. The directional anisotropies are important while comparing theory with experiment as the systematic errors in the experimental and theoretical results are canceled out. The prominent structures near $q=0$ are well reproduced at the correct momentum values; however, they are overestimated by theory (Fig. 3). This is again due to the correlation correction functional as discussed by Bauer and Schneider.[34] In the present calculation, we have included the correlation correction which is isotropic, and therefore does not affect the results of anisotropy. Attempts to include anisotropic corrections are in progress and will be published elsewhere.

The two-dimensional ACPAR surfaces were obtained by integrating $\rho^{2\gamma}(\mathbf{p})$ along ⟨100⟩, ⟨110⟩, and ⟨111⟩ directions, respectively; while the one-dimensional (1D) curves were obtained using the linear tetrahedron method. The 1D ACPAR curves along ⟨100⟩, ⟨110⟩, and ⟨111⟩ directions are shown in Fig. 4, and are in qualitative agreement with earlier published work.[35,36] The 1D ACPAR curves were convoluted with a Gaussian with a FWHM of 0.022 a.u.. The 2D ACPAR data convoluted with 0.5×0.23-mrad^2 FWHM (Ref.

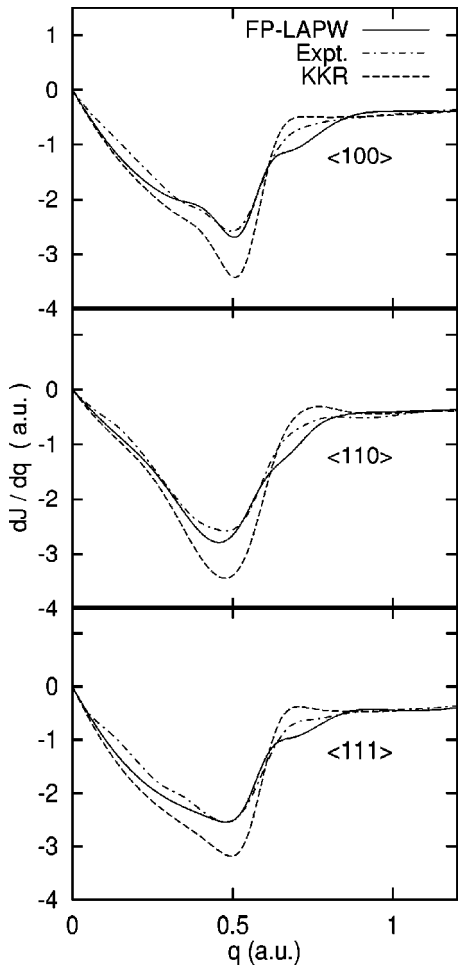

FIG. 6. Derivative of the Compton profiles along ⟨100⟩, ⟨110⟩, and ⟨111⟩ directions.

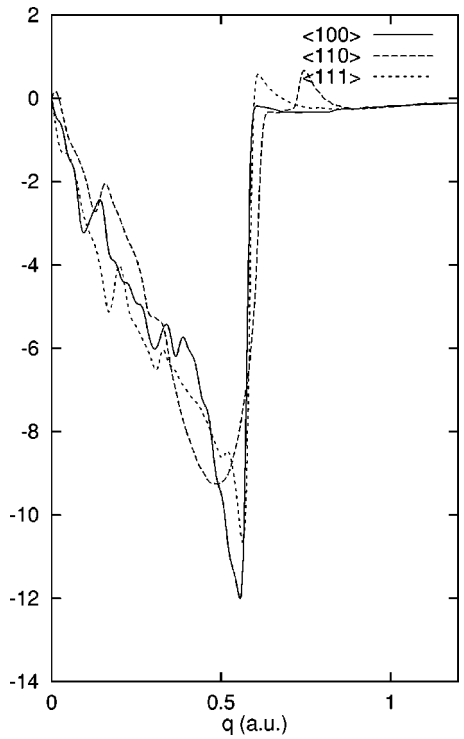

FIG. 7. Derivative of one-dimensional ACPAR curves along ⟨100⟩, ⟨110⟩, and ⟨111⟩ directions.

37) is presented in Fig. 5, and the overall shape matches with experiment.[38] The higher-momentum components in the TPMD are seen quite clearly in the 2D ACPAR plot. The smaller bump comes from the TPMD in the second zone in the ⟨110⟩ direction, whereas the contributions from higher zones are hardly visible. The larger bump is a result of projected contributions from $\langle 01\bar{1}\rangle$ and $\langle 10\bar{1}\rangle$ directions for the same p value. The HMC intensity is seen to be a sharp function of momentum values. The momentum density decreases with increasing momentum values, which is a direct reflection of the *s*-like wave function.

We have extracted relevant FS data from both electron and electron-positron momentum distributions. Although, in principle, both Compton scattering and ACPAR probe the electron momentum distribution and provide complementary information about the FS, the latter provides the best possible measurements for FS breaks in the EMD since the electron-positron correlations enhance the momentum density at k_f. The prominent breaks in momentum distribution are seen around 0.6 a.u. with slightly different values along different directions, as shown in Fig. 1 for the EMD. A similar structure is also seen in the TPMD. The images of the FS breaks, seen in higher zones due to periodicity, are reflected in the CP and ACPAR data. The structures seen are identical to those seen earlier and discussed by Sakurai *et al.*[13] for CP curve and Kim and Stewart[35] for ACPAR curves. However, we point out that the LP correction shifts the FS breaks, as seen in the derivatives of the CP. This is a limitation of the model which employs isotropic momentum density to calculate the LP correction.

Figure 6 displays the first derivatives of the directional Compton profiles. Although the breaks in the first derivative curve without convolution bring out the structures rather well, indicating the distortions of the free-electron sphere; however, in Fig. 6, we show the derivatives of the convoluted Compton profiles to facilitate comparison with experimental results. The derivatives of 1D ACPAR which bring out the FS breaks sharply are presented in Fig. 7. The values of the FS radii along the principal symmetry directions ⟨100⟩, ⟨110⟩, and ⟨111⟩, as estimated from the positions of peaks in the second derivatives of the CP, differ from the actual Fermi radii as described by Sakurai *et al.*[13] The first derivatives of directional ACPAR curves give the correct Fermi radii, since the high-momentum components in the TPMD are smaller. Our values of Fermi radii along with the experimental values,[13] are presented in Table I. The maximum Fermi surface asphericity $[k_{110}-k_{100}]/k_f^0$, where k_f^0 is the free-electron radius, in our calculation turns out to be 5.6% against the experimental value of 4.6%, 5%, and 4.7%,

TABLE I. Values of the Fermi radii.

	Fermi surface radii	
Directions	FP-LAPW	Experiment
k_{1000}	0.578	0.577 ± 0.004
k_{110}	0.611	0.604 ± 0.004
k_{111}	0.585	0.586 ± 0.004

respectively, obtained from CP[13], 1D ACPAR,[39] and 2D ACPAR data.[37]

In this paper, we have presented Compton profiles computed using the FP-LAPW method within the GGA and have corrected them for correlations along the lines of Cardwell and Cooper[25] using self-consistent charge density. The derivatives of the calculated CP's are in good agreement with their experimental counterparts. Usually, the discrepancy between theory and experiment is ascribed to the limitation of the local-density approximation. However, we have seen that gradient corrections to the exchange-correlation potential, as described in the GGA do not affect the electron momentum density significantly. In principle, the Lam-Platzman correction describes the nonlocal effects on the momentum density correctly, but the practical implementation is able to account for it only partly; that is, the isotropic electron correlations are described satisfactorily but not the anisotropic ones. Although Bauer and Schneider[34] rejected the idea of momentum density-functional theory, we feel a description for the exchange-correlation energy functional in momentum space will allow a better quantitative representation of the EMD theoretically.

One- and two-dimensional ACPAR curves are also computed using the FP-LAPW method. We have shown that the different shapes of HMC's are well reproduced by our calculations. Inclusion of a density-dependent enhancement factor is found to reduce HMC's at large p values. To our knowledge, this is the first theoretical report of 1D and 2D ACPAR for Li incorporating density-dependent enhancement effects.

ACKNOWLEDGMENTS

We gratefully acknowledge the experimental data and KKR results provided by Dr. Y. Sakurai and Professor A. Bansil. We are grateful to Professor K. Schwarz and Dr. P. Blaha for providing the WIEN97 code. We are also thankful to Dr. V. Sundarajan and Professor R. M. Singru for helpful discussions. T.B. and R.R.Z. gratefully acknowledge financial support from the Council for Scientific and Industrial Research, New Delhi.

*Author to whom correspondence should be addressed.

[1] *Compton Scattering*, edited by B. G. Williams (McGraw-Hill, London, 1977).
[2] R. M. Singru, in *Positron Annihilation*, edited by P. G. Coleman, S. C. Sharma, and L. M. Diana (North-Holland, Amsterdam, 1982).
[3] R. N. West, in *Positron Annihilation*, edited by P. C. Jain, R. M. Singru, and K. P. Gopinathan (World Scientific, Singapore, 1985).
[4] S. Berko and J. S. Plaskett, Phys. Rev. **112**, 1877 (1958); Positron Annihilation, edited by A. T. Stewart and L. O. Roelling (Academic, New York, 1967); *Positron Studies of Solids, Surfaces and Atoms*, edited by A. P. Mills, Jr., W. S. Crane, and K. F. Canter (World Scientific, Singapore, 1986).
[5] C. K. Majumdar, Phys. Rev. **140**, A227 (1965).
[6] A. B. Migdale, Zh. Eksp. Teor. Fiz. **5**, 399 (1957) [Sov. Phys. JETP **5**, 333 (1957)].
[7] E. Daniel and S. H. Vosko, Phys. Rev. **120**, 2041 (1960).
[8] S. Kahana, Phys. Rev. **129**, 1622 (1963).
[9] P. E. Mijnarends and R. M. Singru, Phys. Rev. B **19**, 6038 (1979).
[10] M. J. Puska, A. P. Seitsonen, and R. M. Nieminen, Phys. Rev. B **52**, 10 947 (1995).
[11] T. Jarlborg and A. K. Singh, Phys. Rev. B **36**, 4660 (1987).
[12] S. Daniuk, G. Kontrym-Sznajd, A. Rubaszek, H. Stachowiak, J. Mayers, P. A. Walters, and R. N. West, J. Phys. F **17**, 1365 (1987).
[13] Y. Sakurai, Y. Tanaka, A. Bansil, S. Kaprzyk, A. T. Stewart, Y. Nagashima, T. Hyodo, S. Nanao, H. Kawata, and N. Shiotani, Phys. Rev. Lett. **74**, 2252 (1995).
[14] M. A. G. Dixon, J. A. Duffy, S. Gardelis, J. E. McCarthy, M. J. Cooper, S. B. Dugdale, T. Jarlborg, and D. N. Timms, J. Phys.: Condens. Matter **10**, 2759 (1998); M. J. Cooper, Radiat. Phys. Chem. **50**, 63 (1997).
[15] W. Schülke, G. Stutz, F. Wohlert, and A. Kaprolat, Phys. Rev. B **54**, 14 381 (1996).
[16] E. E. Lafon and C. C. Lin, Phys. Rev. **152**, 579 (1966).
[17] B. I. Lundqvist and C. Lydén, Phys. Rev. B **4**, 3360 (1971).
[18] P. Eisenberger, L. Lam, P. M. Platzman, and P. Schmidt, Phys. Rev. B **6**, 3671 (1972).
[19] S. Wakoh and J. Yamashita, J. Phys. Soc. Jpn. **35**, 1402 (1973).
[20] W. Y. Ching and J. Callaway, Phys. Rev. B **9**, 5115 (1974).
[21] Y. Kubo, J. Phys. Soc. Jpn. **65**, 16 (1996).
[22] Y. Kubo, J. Phys. Soc. Jpn. **66**, 2236 (1997).
[23] D. Singh, *Planewaves, Pseudopotentials and the LAPW Method* (Kluwer, Boston, 1994).
[24] L. Lam and P. M. Platzman, Phys. Rev. B **9**, 5122 (1974).
[25] D. A. Cardwell and M. J. Cooper, J. Phys.: Condens. Matter **1**, 9357 (1989).
[26] P. Blaha, K. Schwarz, and J. Luitz, WIEN97, Vienna University of Technology, 1997. [Improved and updated Unix version of the original copyrighted WIEN code, which was published by P. Blaha, K. Schwarz, P. Sorantin, and S. B. Trickey, in Comput. Phys. Commun. **59**, 399 (1990).]
[27] J. P. Perdew, S. Burke, and M. Ernzerhof, Phys. Rev. Lett. **77**, 3865 (1996).
[28] *CRC Handbook of Chemistry and Physics*, 74th ed., edited by D. R. Lide (CRC Press, London, 1994).
[29] V. L. Moruzzi, A. R. Williams, and J. F. Janak, *Calculated Electronic Properties of Metals* (Pergamon, New York, 1978).
[30] G. Lehman and M. Taut, Phys. Status Solidi B **54**, 469 (1972).
[31] U. von Barth and L. Hedin, J. Phys. B **16**, 3687 (1983).
[32] L. Lam and P. M. Platzman, Phys. Rev. B **9**, 5128 (1974).
[33] Our work on ferromagnetic Ni, which will be published elsewhere, demonstrates that in Ni the nonlocal corrections affect the EMD. This is in agreement with the results in Ref. 14.
[34] G. E. W. Bauer and J. R. Schneider, Phys. Rev. B **31**, 681 (1985).
[35] S. M. Kim and A. T. Stewart, Phys. Rev. B **11**, 2490 (1975).
[36] J. Meingailis and S. DeBenedetti, Phys. Rev. **145**, 400 (1966).
[37] S. S. Rajput, R. Prasad, R. M. Singru, W. Triftshauser, A. Eckert, G. Kögel, S. Kaprzyk, and A. Bansil, J. Phys.: Condens. Matter **5**, 6419 (1993).
[38] L. Oberli, A. A. Manuel, R. Sachot, P. Descouts, M. Peter, L. P. L. M. Rabou, P. E. Mijnarends, T. Hyodo, and A. T. Stewart, Phys. Rev. B **31**, 1147 (1985).
[39] J. J. Donaghy and A. T. Stewart, Phys. Rev. **164**, 391 (1967).